the parameter a_S a surface tension coefficient σ defined as the surface energy per unit area, and get with Eq. (1.3):

$$\sigma = \frac{a_S}{4\pi r_0^2} = 1.03\ [\mathrm{MeV \cdot fm^{-2}}]. \tag{1.6}$$

The third term takes into account the Coulomb repulsion of the protons. It can be calculated approximately by assuming the charges to be uniformly distributed over a sphere. The *Coulomb energy* of such a system is proportional to the number of proton pairs ($\propto Z^2$) and inversely proportional to the radius.

Since the protons repel one another, it would be energetically more favorable for a nucleus to have only neutrons—if there were no Pauli principle. A proton decaying into a neutron must enter a state above the neutron Fermi level (see Chap. 2), which is energetically unfavored. The energy balance of the neutron excess $N-Z$ is taken care of in the fourth term of Eq. (1.4), the so-called *symmetry energy*. It cannot depend on the sign of $N-Z$. In the Fermi gas model [SF 74, p. 127 f], one can show that it is proportional to $(N-Z)^2/A$. The quadratic dependence of the binding energy on the proton–neutron mass difference is experimentally very well confirmed. Only the base of the experimental parabola is different according to whether we are considering an even–even, even–odd or odd–odd nucleus. This is due to the so-called *pairing effect*, as we shall see in Chapter 6, and is taken care of by the last term in Eq. (1.4).

Some aspects of the semi-empirical mass formula will be discussed again in Chapter 13 in the context of the Thomas–Fermi approach to nuclear physics.

It should be noted that Eq. (1.4) gives only an overall smooth fit to the binding energy as a function of A, and that locally there are strong deviations from it (see Fig. 2.2), mostly due to shell effects, which will be discussed in Section 2.9.

1.3 Deformation Parameters

Up to now, we have only studied static properties of the liquid drop model. In the following, we will assume that the nucleus has a sharp surface* which must not necessarily be spherical, and we imagine it to undergo dynamical shape or surface oscillations.

Before we can investigate these oscillations, we have to parametrize the surface in some way. One possibility is to describe it by the length of the radius vector pointing from the origin to the surface

$$R = R(\theta,\phi) = R_0\left(1 + \alpha_{00} + \sum_{\lambda=1}^{\infty}\sum_{\mu=-\lambda}^{\lambda} \alpha_{\lambda\mu}^{*} Y_{\lambda\mu}(\theta,\phi)\right) \tag{1.7}$$

where R_0 is the radius of the sphere with the same volume. Such a surface

*Myers and Swiatecki [MS 69, 73] have given up this assumption and introduced a refined liquid drop model with a diffuse surface, the so-called "droplet model" [Ni 72].

is certainly not the most general one* but it is widely used and extremely useful for problems of nuclear structure.

The constant α_{00} describes changes of the nuclear volume. Since we know that the incompressibility of the nuclear fluid is rather high, we require that the volume be kept fixed for all deformations as

$$V = \frac{4}{3}\pi R_0^3. \tag{1.8}$$

This defines the constant α_{00}. Up to second order, we get [EG 70]

$$\alpha_{00} = -\frac{1}{4\pi}\sum_{\lambda>1,\,\mu}|\alpha_{\lambda\mu}|^2. \tag{1.9}$$

The term $\lambda = 1$ describes mainly (at least for small deformations) a translation of the whole system. The three parameters $\alpha_{1\mu}$ can be fixed by the condition that the origin coincides with the center of mass

$$\int_V \mathbf{r}\, d^3r = 0. \tag{1.10}$$

If the expansion (1.7) contains only even values of λ, this is fulfilled automatically. Otherwise $\alpha_{1\mu}$ starts with second order in the $\alpha_{\lambda\mu}$ ($\lambda > 2$). Therefore, in the following we omit both α_{00} and $\alpha_{1\mu}$, since we shall restrict our discussion to small deformations.

It is instructive to look at the shapes of lowest multipolarity in the expansion (1.7), as displayed in Fig. (1.3). The deformations corresponding

*For instance, shapes of two separated fragments in the fission process cannot be represented by (1.7), since R is then multivalued.

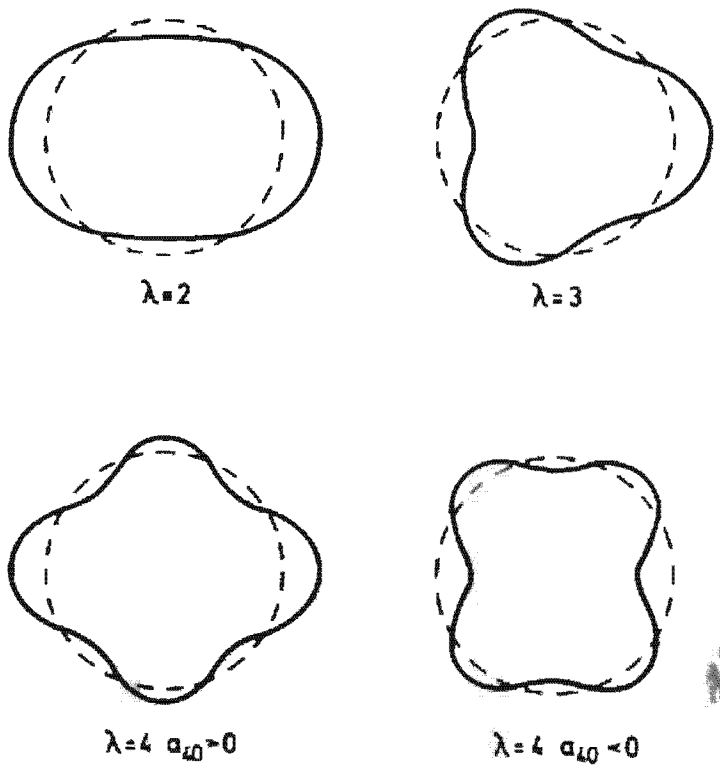

Figure 1.3. Nuclear shapes with quadrupole ($\lambda = 2$), octupole ($\lambda = 3$), and hexadecupole ($\lambda = 4$) deformations.

to $\lambda=2$ look like ellipsoidal deformations. It should be noticed, however, that this is true only up to first order. A pure ellipsoid has non-vanishing $\alpha_{\lambda\mu}$ for all $\lambda \geqslant 2$.

Another condition on R, and therefore on the parameters $\alpha_{\lambda\mu}$, is the fact that R should be invariant under a reflection of the coordinate system and under a rotation of the coordinate system. In order for this to be the case, the $\alpha_{\lambda\mu}$ must be multiplied by a factor $(-)^{\lambda}$ under a parity transformation, and must behave like $Y_{\lambda\mu}(\theta,\phi)$ under a rotation of the coordinate system (characterized by the Euler angles $\Omega=(\alpha,\beta,\gamma)$ [Ed 57, Eq. (5.2.1.)]), i.e.,

$$(Y_{\lambda\mu})_{\text{new}}=\sum_{\mu'} D^{\lambda}_{\mu'\mu}(\Omega)(Y_{\lambda\mu'})_{\text{old}}, \tag{1.11}$$

$$a_{\lambda\mu}=\sum_{\mu'} D^{\lambda}_{\mu'\mu}(\Omega)\alpha_{\lambda\mu'},$$

where $D^{\lambda}_{\mu'\mu}(\Omega)$ are the Wigner functions of the rotation and $a_{\lambda\mu}$ are the deformation parameters in the new system.

To make sure that the radius R in Eq. (1.7) is real, we have to use the property $Y^{*}_{\lambda\mu}=(-)^{\mu}\cdot Y_{\lambda-\mu}$, and get

$$\alpha^{*}_{\lambda\mu}=(-)^{\mu}\alpha_{\lambda-\mu}. \tag{1.12}$$

This will turn out to be the time reversal behavior of the $\alpha_{\lambda\mu}$'s.

Before discussing the surface oscillations of general multipolarity, we mention two special cases:

(i) First are the axially symmetric deformations. Choosing the z-axis as symmetry axis, we find that $\alpha_{\lambda\mu}$ vanishes except when $\mu=0$. The deformation parameters $\alpha_{\lambda 0}$ are usually called β_{λ}.

(ii) In the case of quadrupole deformations ($\lambda=2$), we have five parameters $\alpha_{\lambda\mu}$. Not all of them describe the shape of the drop. Three determine only the orientation of the drop in space, and correspond to the three Euler angles. By a suitable rotation, we can transform to the body-fixed system characterized by three axes 1, 2, 3, which coincide with the principal axes of the mass distribution of the drop. The five coefficients $\alpha_{2\mu}$ reduce to two real independent variables a_{20} and $a_{22}=a_{2-2}$ ($a_{21}=a_{2-1}=0$), which, together with the three Euler angles, give a complete description of the system. It is convenient to introduce instead of a_{20} and a_{22} the so-called Hill–Wheeler [HW 53] coordinates β,γ ($\beta>0$) through the relation

$$a_{20}=\beta\cdot\cos\gamma,$$

$$a_{22}=\frac{1}{\sqrt{2}}\cdot\beta\cdot\sin\gamma, \tag{1.13}$$

from which we have

$$\sum_{\mu}|\alpha_{2\mu}|^{2}=a_{20}^{2}+2a_{22}^{2}=\beta^{2} \tag{1.14}$$

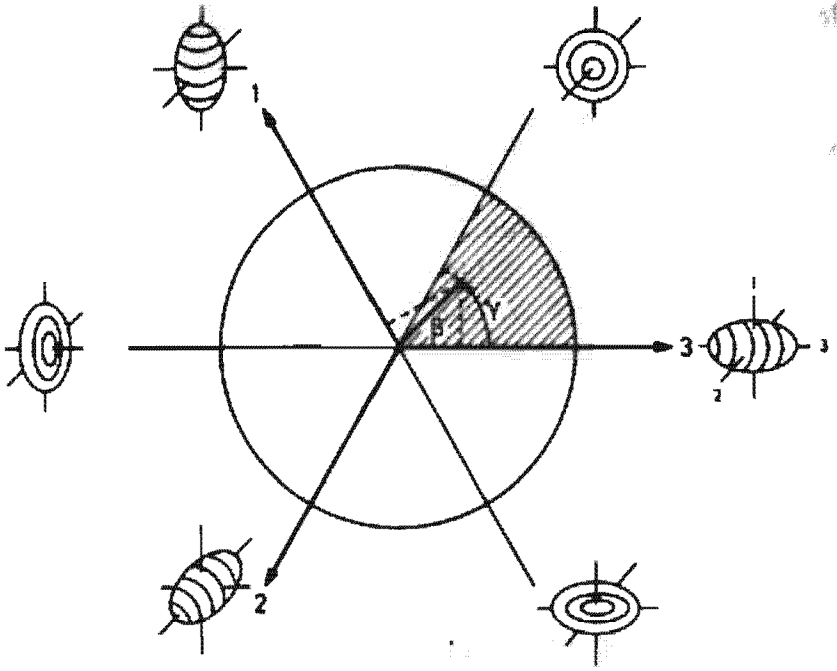

Figure 1.4. Nuclear shapes in the β, γ plane. The projections onto the three axes are proportional to the increments of δR_x (1.16).

and

$$R(\theta,\phi)=R_0\left\{1+\beta\sqrt{\frac{5}{16\pi}}\left(\cos\gamma(3\cos^2\theta-1)\right.\right.$$
$$\left.\left.+\sqrt{3}\sin\gamma\sin^2\theta\cos 2\phi\right)\right\}. \tag{1.15}$$

In Fig. (1.4) the $\lambda=2$ shapes are represented in the polar coordinates β, γ. We see that

(i) γ values of 0°, 120°, and 240° yield prolate spheroids with the 3, 1 and 2 axes as axes of symmetry;
(ii) $\gamma=180°$, 300°, and 60° lead to the corresponding oblate shapes
(iii) when γ is not a multiple of 60° it corresponds to a triaxial shape;
(iv) there are discrete symmetries, namely, one can interchange all three axes without changing the shape, which means an invariance under the point group D_2. The interval $0<\gamma<60°$ is sufficient to describe all the $\lambda=2$ shapes. All other points in Fig. 1.4 are obtained by suitable exchanges of the different axes.
(v) We can calculate the increments of the three semi-axes in the body-fixed frame as functions of β and γ:

$$\delta R_1=R\left(\frac{\pi}{2},0\right)-R_0=R_0\sqrt{\frac{5}{4\pi}}\ \beta\cos\left(\gamma-\frac{2\pi}{3}\right),$$

$$\delta R_2=R\left(\frac{\pi}{2},\frac{\pi}{2}\right)-R_0=R_0\sqrt{\frac{5}{4\pi}}\ \beta\cos\left(\gamma+\frac{2\pi}{3}\right),$$

$$\delta R_3=R(0,0)-R_0=R_0\sqrt{\frac{5}{4\pi}}\ \beta\cos\gamma,$$

or

$$\delta R_\kappa = R_0 \sqrt{\frac{5}{4\pi}}\ \beta \cos\left(\gamma - \frac{2\pi}{3}\kappa\right), \qquad \kappa = 1, 2, 3. \tag{1.16}$$

We have to remember, however, that the parameters β and γ (with (1.7)) only describe exactly ellipsoidal shapes in the limit of small β-values (see also Eq. 1.88).

1.4 Surface Oscillations About a Spherical Shape

The first kind of excitations are dynamical shape, or surface, oscillations. The dynamical variables are in this case the parameters which describe the surface, i.e., the surface coordinates $\alpha_{\lambda\mu}$ ($\lambda \geqslant 2$) of Eq. (1.7). They are considered to be functions of time: $\alpha_{\lambda\mu}(t)$. For the low-lying excitations one can expect that they produce small oscillations around the spherical equilibrium shape with $\alpha_{\lambda\mu} = 0$, and that the classical Hamilton function H_{coll} that describes this process is of a harmonic oscillator form [Bo 52]:

$$H_{\text{coll}} = T + V = \frac{1}{2} \sum_{\lambda,\ \mu} \left\{ B_\lambda |\dot{\alpha}_{\lambda\mu}|^2 + C_\lambda |\alpha_{\lambda\mu}|^2 \right\}, \tag{1.17}$$

Here the parameters of inertia B_λ and of stiffness C_λ are real constants. This is, in fact, the only quadratic form which is invariant under rotation and time reversal.*

Following the usual rules of canonical quantization (see for instance, [EG 70, p. 40]), we obtain the quantized form† (see also Appendix C)

$$\hat{H}_{\text{coll}} = \sum_{\lambda\mu} \hbar\Omega_\lambda \left(B^+_{\lambda\mu} B_{\lambda\mu} + \frac{1}{2} \right) \tag{1.18}$$

with the frequencies

$$\Omega_\lambda = \left(\frac{C_\lambda}{B_\lambda} \right)^{1/2}. \tag{1.19}$$

The operators $B_{\lambda\mu}$ obey Bose commutation rules

$$\left[B_{\lambda\mu}, B_{\lambda'\mu'} \right] = 0; \qquad \left[B_{\lambda\mu}, B^+_{\lambda'\mu'} \right] = \delta_{\lambda\lambda'} \delta_{\mu\mu'} \tag{1.20}$$

and have a corresponding Bose vacuum $|0)$ such that $B_{\lambda\mu}|0) = 0$. The Boson operators $B_{\lambda\mu}$ are related to the coordinates $\hat{\alpha}_{\lambda\mu}$ and corresponding momenta $\hat{\pi}_{\lambda\mu}$ by

$$\hat{\alpha}_{\lambda\mu} = \left(\frac{\hbar}{2B_\lambda \Omega_\lambda} \right)^{1/2} \left(B^+_{\lambda\mu} + (-)^\mu B_{\lambda-\mu} \right), \tag{1.21}$$

$$\hat{\pi}_{\lambda\mu} = i \left(\frac{\hbar}{2} B_\lambda \Omega_\lambda \right)^{1/2} \left((-)^\mu B^+_{\lambda-\mu} - B_{\lambda\mu} \right).$$

*The time reversal operation is discussed in great detail by Messiah [Me 61] and it is shown that in a system without spin, as we have here, time reversal corresponds to complex conjugation.

†One should not mix up the boson operators $B_{\lambda\mu}$ with the inertia parameters B_λ.

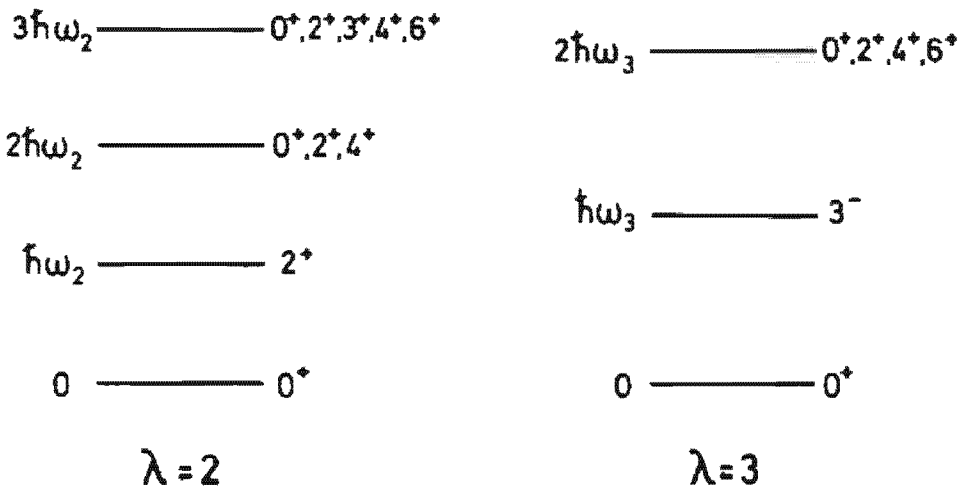

Figure 1.5. Harmonic energy spectra for the quadrupole ($\lambda=2$) and octupole ($\lambda=3$) surface oscillations.

From the above considerations, it follows that for each λ we have a harmonic spectrum of surface vibrations as illustrated in Fig. 1.5.

From the fact that $\alpha_{\lambda\mu}$ and $B^+_{\lambda\mu}$ behave like spherical tensors under rotations of the coordinate system (Eq. (1.11), [Ed 57, Eq. (5.2.1)]) we know the commutation relations of the angular momentum operators with $B^+_{\lambda\mu}$ and find that the one-boson states

$$|\lambda\mu) = B^+_{\lambda\mu}|0) \tag{1.22}$$

have angular momentum $I=\lambda$ and z-component $M=\mu$ with parity $(-)^\lambda$.

To construct multi-boson states we have to use the rules of angular momentum coupling [Ed 57] and also have to take into account that states with more than two bosons are symmetric under the exchange of any two of them. For instance, we get, for the superposition of two quadrupole bosons ($\lambda=2$), the three combinations $I^\pi=0^+,2^+,4^+$

$$|IM) = \frac{1}{\sqrt{2}} \sum_{\mu_1\mu_2} C^{2\ 2\ I}_{\mu_1\mu_2 M} B^+_{2\mu_1} B^+_{2\mu_2}|0). \tag{1.23}$$

The states with $I=1,3$ vanish identically because of the behavior of the Clebsch–Gordan coefficients* [Ed 57, Eq. (3.5.14)]

$$C^{2\ 2\ I}_{\mu_1\mu_2 M} = (-)^I C^{2\ 2\ I}_{\mu_2\mu_1 M},$$

under an exchange of μ_1 and μ_2.

Indeed, many spherical nuclei show in their spectrum a low-lying 2^+ state and, at roughly double the excitation energy, a so-called two-boson triplet ($0^+,2^+,4^+$) which is, however, usually split up a little (see Fig. 9.4).

The constants B_λ and C_λ can be calculated within the fluid picture; they depend on the flow associated with the surface oscillations. Therefore, it is necessary to postulate the nature of the fluid motion within the drop. At this point we should again discuss what the concept of a nuclear fluid

* We use the symbol $C^{j_1 j_2 j_3}_{m_1 m_2 m_3}$ which is the same as $(j_1 m_1 j_2 m_2 | j_1 j_2 j_3 m_3)$.

implies. In Chapter 13 we will investigate this point in detail and show that the fact that the nucleus is a Fermi liquid and not an ordinary liquid plays an important role. The simplest assumption about the flow pattern of the fluid we can make is that it is irrotational, i.e., $\mathbf{rot}\,\mathbf{v}(\mathbf{r})=0$, where $\mathbf{v}$ is the velocity field. We shall also study the justification of this point in Chapter 13, but for the moment let us take it for granted and thus have:

$$\mathbf{v}(\mathbf{t}) = -\nabla\Phi(\mathbf{r}). \tag{1.24}$$

The next assumption is that of *incompressibility*, which is quite well justified for nuclei. It means that the density inside the nucleus is constant ($\dot{\rho}=0$), and we get from the equation of continuity

$$\nabla\mathbf{v}=0 \tag{1.25}$$

and, from (1.24),

$$\Delta\Phi=0. \tag{1.26}$$

The most general solution of Eq. (1.26) regular at the origin can be written in the form

$$\Phi(\mathbf{r}) = \sum_{\lambda\mu} d^*_{\lambda\mu} r^\lambda Y_{\lambda\mu}(\theta,\phi). \tag{1.27}$$

For small deformations we have the boundary condition that the radial component of the velocity is, in lowest order, given by:

$$v_r = -\frac{\partial}{\partial r}\Phi = \dot{R} \qquad \text{at} \quad r=R_0,$$

which, with Eq. (1.7), yields the following relation between the coefficients $d_{\lambda\mu}$ and $\alpha_{\lambda\mu}$.

$$d_{\lambda\mu} = -\frac{1}{\lambda} R_0^{2-\lambda}\dot{\alpha}_{\lambda\mu}. \tag{1.28}$$

The kinetic energy of the surface vibrations is given by

$$T = \frac{m}{2}\rho\int_V \mathbf{v}^2(\mathbf{r})\,d^3r = \frac{m}{2}\rho\int_V |\nabla\Phi|^2\,d^3r = \frac{m}{2}\rho\oint_S \Phi^*\nabla\Phi\,d\mathbf{s},$$

where ρ is the constant density of nucleons with the mass m. Using the gradient formula for spherical harmonics [Ed 57, Eq. (5.9.17)] and [Ed 57, Eqs. (5.9.13) and (5.9.16)] we arrive in the approximation of small deformations (integrating over a sphere), in the following expression for the kinetic energy.

$$T = \frac{R_0^5 m\rho}{2}\sum_{\lambda\mu}\frac{|\dot{\alpha}_{\lambda\mu}|^2}{\lambda}. \tag{1.29}$$

Comparison with (1.17) yields the mass parameter

$$B_\lambda = \frac{\rho m R_0^5}{\lambda} = \frac{3}{4\pi\lambda} A\cdot m R_0^2. \tag{1.30}$$

For oscillations about a spherical equilibrium shape the mass parameter is not a function of μ; this would not be so for a deformed nuclear drop.

The potential energy of a liquid drop with a surface deformation characterized by the parameters $\alpha_{\lambda\mu}$ can be obtained from the coefficients of the Bethe-Weizsäcker formula (1.4) if we neglect changes of the symmetry and pairing energy with deformation.

Because of the assumption of incompressibility, it is tempting to say that the volume term does not depend on the deformation. This is, however, only true for ordinary fluids, and we will see in Chapter 13 how in quantum fluids the volume term can depend on α in a quite subtle fashion. In the usual treatment of the liquid drop model [BM 53, EG 70], however, the volume term is not taken into account, and therefore the deformation energy has only two parts, resulting from the surface and Coulomb terms in Eq. (1.4). As we will discuss in more detail in Chapter 13 this will be sufficient for the monopole and the dipole resonance but not for resonances of other multipolarities.

The deformation energy is defined as the difference between the energy of the deformed and spherical drop:

$$V(\alpha) = E_S(\alpha) - E_S(0) + E_C(\alpha) - E_C(0). \tag{1.31}$$

The surface energy is given by the product of the surface with the surface tension σ [Eq. (1.6)]. With techniques similar to those used in the derivation of Eq. (1.29), we find up to second order in $\alpha_{\lambda\mu}$ [Wi 64, Chap. 2]:

$$E_S(\alpha) = \sigma \oint_S ds = E_S(0) + \frac{1}{2} \sum_{\lambda\mu} (\lambda - 1)(\lambda + 2) R_0^2 \sigma |\alpha_{\lambda\mu}|^2. \tag{1.32}$$

The Coulomb energy E_C is the sum of interactions between pairs of volume elements d^3r_1 and d^3r_2 [Wi 64]

$$E_C(\alpha) = (Ze)^2 \int_V \int \frac{d^3r_1 d^3r_2}{|\mathbf{r}_1 - \mathbf{r}_2|} = E_C(0) - \frac{1}{2} \sum_{\lambda\mu} \frac{3(\lambda - 1)(Ze)^2}{2\pi(2\lambda + 1) R_0} |\alpha_{\lambda\mu}|^2. \tag{1.33}$$

From (1.32), (1.33), and (1.17), we thus get the stiffness coefficients ($\lambda \geq 2$):

$$C_\lambda = (\lambda - 1)(\lambda + 2) R_0^2 \sigma - \frac{3(\lambda - 1)}{2\pi(2\lambda + 1)} \frac{(Ze)^2}{R_0}. \tag{1.34}$$

In principle, we are now able to calculate nuclear spectra from Eq. (1.19) and the coefficients B_λ and C_λ. It turns out, however, that the reproduction of spectra is not the most sensitive test for a nuclear model. A quantum mechanical state is represented by a wave function. Electromagnetic moments and transition probabilities depend strongly on the wave functions and provide a much better test. We therefore first discuss such quantities before comparing the theory with experimental data.

In Appendix B the calculation of the electromagnetic properties of a nucleus is shown. The essential quantities are the electric and magnetic multipole operators.

The electric multipole operators are in the limit of long wavelengths (low transition energies) given by [Eq. (B.18)]

$$\hat{Q}_{\lambda\mu} = e \int_V \rho_p(\mathbf{r}) r^\lambda Y_{\lambda\mu}(\theta, \phi)\, d^3r.$$

We can express them by the cordinates $\alpha_{\lambda\mu}$, taking in the integral a constant proton density ρ_p for a shape defined by Eq (1.7) and get

$$\hat{Q}_{\lambda\mu} = \rho_p \cdot e \cdot \int_{4\pi} d\cos\theta\, d\phi\, Y_{\lambda\mu}(\theta,\phi) \frac{1}{\lambda+3} R^{\lambda+3}(\theta,\phi),$$

which is up to second order in $\alpha_{\lambda\mu}$ (with [Ed 57, Eq. (4.6.3)])

$$\hat{Q}_{\lambda\mu} = \frac{3e}{4\pi} Z R_0^{\lambda} \left\{ \hat{\alpha}_{\lambda\mu} + \frac{1}{2}(\lambda+2) \sum_{\lambda_1\mu_1} \sum_{\lambda_2\mu_2} \hat{\alpha}_{\lambda_1\mu_1} \hat{\alpha}_{\lambda_2\mu_2} (-)^{\mu} \right.$$

$$\left. \cdot \sqrt{\frac{(2\lambda_1+1)(2\lambda_2+1)(2\lambda+1)}{4\pi}} \begin{pmatrix} \lambda_1 & \lambda_2 & \lambda \\ 0 & 0 & 0 \end{pmatrix} \begin{pmatrix} \lambda_1 & \lambda_2 & \lambda \\ -\mu_1 & -\mu_2 & \mu \end{pmatrix} \right\}. \quad (1.35)$$

The magnetic multipole operators are given by [Eq. (B. 22)]

$$\hat{M}_{\lambda\mu} = \frac{1}{c(\lambda+1)} \int_V (\mathbf{r} \times \mathbf{j}(\mathbf{r})) \left(\nabla r^{\lambda} Y_{\lambda\mu} \right) d^3r.$$

As in the case of the mass parameters, we could again use the assumption of irrotational flow to define the current density $\mathbf{j}$ and express $\hat{M}_{\lambda\mu}$ by $\alpha_{\lambda\mu}$ and $\dot{\alpha}_{\lambda\mu}$ (see [Da 68, Chap. 6]). However, we will restrict ourselves to the case of $M1$ operators, which form a vector

$$\hat{\mathbf{M}}1 = \sqrt{\frac{3}{4\pi}}\ \hat{\boldsymbol{\mu}}.$$

Since we have no spins in the system, we get for the magnetic dipole moment

$$\hat{\boldsymbol{\mu}} = \frac{1}{2c} \int_V (\mathbf{r} \times \mathbf{j})\, d^3r = \frac{Z}{A} \frac{e}{2mc} \int_V (\mathbf{r} \times m\mathbf{v})\, d^3r = \frac{Z}{A} \frac{e\hbar}{2mc} \hat{\mathbf{I}} = g_R \hat{\mathbf{I}} \mu_N \quad (1.36)$$

with the gyromagnetic ratio of the rotor

$$g_R = \frac{Z}{A}. \quad (1.37)$$

The calculation of lifetimes and transition probabilities requires the knowledge of $BE\lambda$- and $BM\lambda$-values [see Eq. (B. 73)] defined by

$$B\left(\left\{ \begin{matrix} E \\ M \end{matrix} \right\} \lambda, I_i \to I_f \right) = \frac{1}{2I_i+1} \left| < I_f \| \left\{ \begin{matrix} \hat{Q}_{\lambda} \\ \hat{M}_{\lambda} \end{matrix} \right\} \| I_i > \right|^2. \quad (1.38)$$

Since the $M1$-operator (1.36) conserves angular momentum, $M1$-transitions are forbidden in this model. The most important transitions are $E2$-transitions.

As an example, we calculate the $BE2$-value for the transition from the one-boson state $B^+_{2\mu}|0)$ to the ground state $|0)$. Expressing $\hat{\alpha}_{2\mu}$ by the operators $B_{2\mu}$ and $B^+_{2\mu}$ (1.21), and using the wave function (1.22), we get to first order in the $\alpha_{2\mu}$'s

$$B(E2, 2_1^+ \to 0^+) = \left(\frac{3}{4\pi} Z e R_0^2 \right)^2 \frac{\hbar}{2B_2\Omega_2}. \quad (1.39)$$

Before we compare these theoretical results of our model with experimental data, we must discuss which levels in the excitation spectra of nuclei would be appropriate candidates for such surface vibrations. We restrict the following discussion to 2^+ states. For other angular momenta similar considerations apply.

Figure 1.6 shows schematically the structure of the 2^+ spectra. They have a discrete part and a continuum with resonances. Among the discrete lines one 2^+ level is usually very low in energy. With a few exceptions it is the lowest excited state in each nucleus and, as shown in Fig. 1.6, it carries a large $BE2$ value, i.e., it has a high transition probability to the ground state (see Appendix B). The measured $BE2$ values are for spherical nuclei roughly ten to twenty times larger than one would expect from a pure single-particle transition [Weisskopf unit, see Eq. (B. 85)].

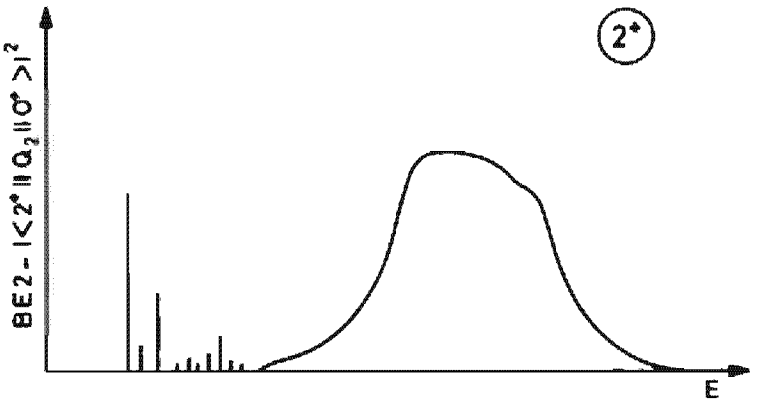

Figure 1.6. Schematic representation of the 2^+ spectra in nuclei. The ordinate gives the $BE2$ values for the discrete levels and the density of the $BE2$ strength in the resonance region. These quantities measure the transition probability to the ground state. The units are arbitrary.

The low-lying 2^+ states therefore have collective character, i.e., many particles contribute and they have very often been interpreted as surface quadrupole vibrations. Figure (1.7) shows the energy E_{2^+} for the lowest 2^+ state in even–even nuclei. One observes large shell effects (see Chap. 2). Only the average trend is given by the liquid drop model with irrotational flow [Eqs. (1.19) (1.30) and (1.34)]. The absolute value is off by a factor of five. The reason for this failure will become clear below.

Experimentally, it has been found that there is a strong correlation between the $BE2$ value of the first 2^+ state and its energy $E_{2_1^+} = \Omega_2$ [Gr 62]:

$$E_{2_1^+} B(E2, 2^+ \to 0^+) \simeq (25 \pm 8) \frac{Z^2}{A} \left[\text{MeV } e^2 \text{ fm}^4\right]. \tag{1.40}$$

This empirical relation holds for all the nuclei throughout the nuclear table. Equation (1.39) shows the same energy dependence, but the A dependence is different.The strong shell effects in the low-lying 2^+ states indicate that they cannot be pure quadrupole surface oscillations and that there are other states which also have the character of such collective vibrations. From Eqs. (1.22), (1.21), and (1.35) we see that the quadrupole

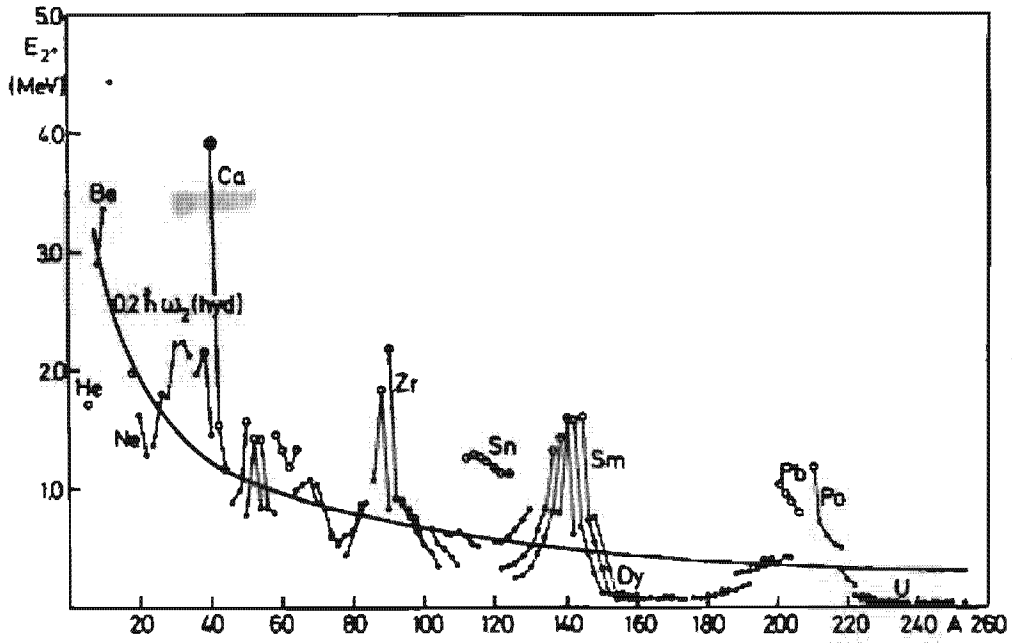

Figure 1.7. The energy of the first 2^+ state in even–even nuclei. The nuclei with closed neutron or proton shells are marked by open circles. (From [NN 65].)

surface vibration can be represented in linear order in α as:

$$|2\mu) = B^+_{2\mu}|0) \propto \hat{\alpha}_{2\mu}|0) \propto \hat{Q}_{2\mu}|0). \tag{1.41}$$

The overlap of an arbitrary state $|\nu\rangle$ with the quadrupole surface vibration is therefore proportional to its $BE2$ value:

$$|\langle \nu | 2\mu\rangle|^2 \propto |\langle \nu|\hat{Q}_{2\mu}|0\rangle|^2 \propto B(E2, \nu \to 0). \tag{1.42}$$

and the probability that it can be interpreted as such a vibration is given by the percentage to which it exhausts the sum rule

$$S^0_{2\mu} = \sum_{\nu \neq 0} |\langle \nu|\hat{Q}_{2\mu}|0\rangle|^2. \tag{1.43}$$

Only if one state exhausts this sum rule to a large extent is it meaningful to call it a quadrupole surface vibration.

In Section 8.7 we will discuss in great detail the sum rules and how they can be evaluated. It is evident that in a model where the state $\hat{Q}_{\lambda\mu}|0\rangle$ is an eigenstate of the system, like the model we are now investigating, this state exhausts the sum rules completely, because all the other states are orthogonal to it.

Experimentally, it has been found that the low-lying 2^+ state usually exhausts about 10–20% of the sum rule. The major part is exhausted by the resonances in the continuum [see Fig. (1.6)], the so-called giant resonances.

Such giant resonances for different I values have been observed. The most famous is the giant dipole resonance (1^-) which has been well known since more than 30 years and lies at an energy (see Fig. 1.8) (for more details see Chap. 13):

$$\Omega^{GR}_{1^-} \simeq 77 \cdot A^{-1/3 + -1/6}\,[\text{MeV}]. \tag{1.44}$$

As we shall see in Chapters 8 and 13, it corresponds to a vibration of the neutron and proton sphere against one another and cannot be described in the present simple model.

In the last ten years, further giant resonances have been observed. The most important example is the isoscalar giant quadrupole resonance. It lies at (see Fig. 1.8)

$$\Omega_{2^+}^{GR} \simeq 62 \cdot A^{-1/3} \,[\mathrm{MeV}] \tag{1.45}$$

and exhausts in most cases a major part of the S_{2^+} sum rule.

It seems, therefore, to be more reasonable to interpret this resonance as the quadrupole surface vibration mode discussed so far. The liquid drop model in this form is, however, not able to give the proper A-dependence. From Eqs. (1.19), (1.30), and (1.34) we get

$$\Omega_2 \propto A^{-1/2},$$

which does not agree with the experimental value (1.45). In Chapter 13 we will see that the reason for this deviation comes from the fact that the potential energy coefficients C_λ correspond to the total binding energy of the liquid drop [(1.31), (1.34)]. This total binding energy is, however, a sum of intrinsic kinetic and potential energy. The fact that (at least, for small deformations) the intrinsic kinetic energy depends on the deformation has been neglected in (1.34). This can be understood simply as an effect of the long mean free path of the nucleons and the uncertainty principle, which states that in an ellipsoidal shape the nucleons along the short axis have higher momenta than those along the long axis. An ellipsoidal momentum distribution, however, yields a larger kinetic energy than a spherical one. Since all particles are affected, it is a volume effect which dominates in general over the surface dependence given in (1.34). In Chapter 13 we will give a detailed discussion of this point.

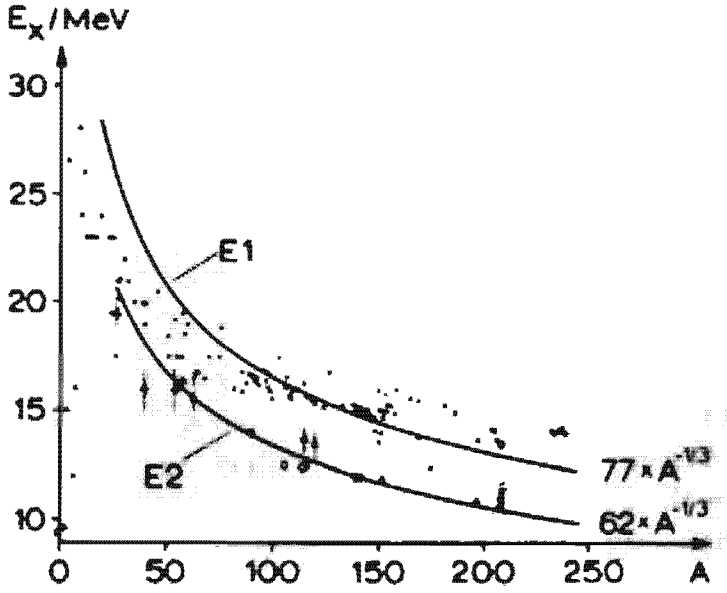

Figure 1.8. The energy of the giant dipole and the isoscalar giant quadrupole resonance as a function of mass number [Wa 73].

In spite of these deficiencies, the boson model presented so far has been extensively used over the years and has proved quite successful in explaining many features of the nuclear spectra [EG 70]. The reason for this is that many low-lying nuclear excitations have a rather collective character and can be represented to a good approximation as bosons. The parameters B_λ and C_λ may not be given very well in the liquid drop model, but, as we will shown in Chapters 8 and 9, there are microscopic theories for fermions which allow more reliable calculations of B_λ and C_λ; therefore, we should consider B_λ and C_λ more as open adjustable parameters than as determined by the LDM.

The microscopic theories also will show that the harmonic approximations (1.17) have only a very rough validity in the limit of very small vibrations. For collective motions with larger amplitudes, one has to take into account anharmonic terms such as

$$\alpha^4, \alpha^2 \cdot \dot{\alpha}^2, \dot{\alpha}^4, \ldots .$$

Again the corresponding parameters can be adjusted to experiment or calculated from a microscopic many-body theory (see Chap. 9).

1.5 Rotations and Vibrations for Deformed Shapes

1.5.1 The Bohr Hamiltonian

The pure liquid drop model has a stable equilibrium only for spherical surfaces. As we shall see later (Sec. 2.8) it can happen as a consequence of quantum mechanics—i.e., shell effects—that the potential $V(\alpha)$ in the collective Hamiltonian has minima at finite non-vanishing values of $\alpha = \alpha_0$. In such cases the nucleus can have a stable ground state deformation.

In this case, the nucleus can exhibit *rotations* which can be described by time-dependent surface parameters $\alpha_{\lambda\mu}$ in the laboratory frame. We shall call these rotations collective ones: This kind of rotation will not be possible around an axis of symmetry, because we cannot distinguish the rotated system from the original one in our variables $\alpha_{\lambda\mu}$.

In a quantum mechanical description, a system with an axis of symmetry (for example, the z-axis) is given by a wave function which is an eigenfunction of the angular momentum operator J_z, and any rotation about this axis produces only a phase. The rotating system has, therefore, the same wave function as the ground state, and the same energy.

This does not mean that there are no other degrees of freedom in the system that can be excited (for instance, single-particle degrees of freedom) and carry angular momentum parallel to the symmetry axis. Such a "rotation," however, we do not call collective rotation.

Since in almost all nuclei the quadrupole degree of freedom plays a fundamental role, we will restrict the following considerations to the case $\lambda = 2$.